Indian Journal of Biochemistry & Biophysics
Vol. 57, June 2020, pp. 283-290

Structural insights on Sucrose transport by *Oryza sativa* L. Sucrose/H^+ Symporter1 (OsSUT1) through refined sequence - template alignment based structural modelling

Divya P Syamaladevi[1]* & Bhagyashree Biswal[1,2]

[1]ICAR-Indian Institute of Rice Research, Hyderabad-500 030, Telangana, India
[2]Siksha O Anusandhan University, Bhuvaneshwar-751 030, Odisha, India

Received 20 September 2019; *revised 04 March 2020*

Sucrose/H^+ Symporters (SUTs) play an important role in plant growth and yield. They are involved in long– distance transport of sucrose from source leaves to filling grains of cereals through a process called phloem loading. However, the molecular mechanism of sucrose transport through SUTs is not yet known. Understanding the key residues involved in sucrose transport can be helpful in developing high yielding varieties through genetic engineering, gene editing or allele mining. Here, the molecular model of OsSUT1 developed based on refined target-template alignment using Modeller software provides structural insights on the sucrose transport mechanism. We propose 13 putative sucrose binding residues and 11 putative H^+ binding residues involved in sucrose/H^+ co-transport in OsSUT1.

Keywords: Phloem loading, Rice SUT, Molecular modelling, SUT structure

Sucrose is the transport form of assimilates in plants and its transport is a vital process associated with plant growth and development[1]. Sucrose transporters of the family SUT/SUC are members of the Majour Facilitator Superfamily (MFS)[2]. They translocate sucrose from the leaves to the grains and growing parts through a process known as phloem loading[3-5]. SUTs are sucrose/H^+ symporters transport sucrose against its concentration gradient. For this, SUTs use the proton motive force (PMF) present across the plasma membrane of the sieve element – companion cell complex[2,3,6-10].

There are different SUTs (SUT1-5) functioning in different tissues and environmental conditions[12-14]. In rice, SUT1 is active in the tissues of long– distance

known to affect yield directly . Knock down and gene expression experiments have revealed the role of SUTs in growth and yield of crops like rice[18,19], wheat[20] , maize[21,22] , tobacco[23] and potato[24].

Even though some MFS members are functionally well characterized[25], the insights on SUT function are limited due to lack of crystal structures. Understanding the molecular mechanism of sucrose transport through SUTs is an important step towards the genetic manipulation of crop varieties for high yield.

SUTs are predicted to be 12-helix trans-membrane proteins with two hexa helical halves[2,8]. The interaction between the two separately expressed halves of SUT1 was detected by an optimized split-ubiquitin system and a schematic model of interaction was proposed[8]. In OsSUT1, R188 has been identified as functionally important and additional binding sites have been attributed to the ites[26]. However, the atomic level intra and intermolecular interactions determining the substrate selectivity, transport and higher–order organization of SUTs are not much studied.

The crystal structure of lactose permease, a 12-helix transporter of the MFS family, suggests that the interface between the two hexa-helical halves makes the lactose channel[27]. Similar to lactose permease, SUT also transports chargeless polar metabolite. Therefore, the models of SUTs using lactose permease as template can provide details on its molecular function. As the target-template

*Correspondence:
Phone: +91 40 24591224
Fax: +91 40 24591217
E-mail:dpsdevi@gmail.com

Abbreviations: Asp, Aspartic acid; Glu, Glutamic acid; MFS, Major Facilitator Superfamily; SUT, Sucrose Transporter; TM helix, Trans-Membrane Helix

Suppl. Data available on respective page of NOPR

alignment quality determines the reliability of the model, we developed and evaluated six different models of OsSUT1 based on different sequence-template alignments to arrive at a most likely model of OsSUT1.

Materials and Methods

Gene threading and target- template alignment

In the absence of homologous structures of OsSUT1, the closest structural templates were identified by gene threading using the Phyre2 server (http://www.sbg.bio.ic.ac.uk/phyre2/html/page.cgi?id=index)[28]. From the templates identified with 100% confidence, two were considered for homology modelling using Modeller 9.19[29]. Six alternate target-template sequence alignments were generated for homology modelling. First, sequence alignment between 1PV7 (lactose permease - template) and OsSUT1 (target) was performed using clustalW[32] and the resulted alignment was called raw alignment or alignment 1. Alignment 2 is a refined form of the raw alignment and was developed using a piecemeal alignment approach wherein the trans-membrane (TM) regions were re-aligned keeping the conserved short motifs at the loop boundaries fixed (Suppl. File 1). Wherever the short motifs at loop boundaries were evident, (as in NFE at loop4, NNQ at loop5, FRQ at loop 6 and FATs at loop7 and loop 9) they were brought in to register. Alignment 3 was made from alignment 2 by redefining the loop boundaries that showed too many unfavourable interactions (clashes) in the alignment 2 based model. Alignment 4 was developed based on HMMTop predicted TM helix boundaries. Alignment 5 and Alignment 6 are as provided by Phyre 2 server for templates 1PV7 and 3WDO respectively. Alignments were visualized using Jalview[31].

Modelling and mapping of interatomic clashes

Separate homology modelling experiments were performed for each alignment. A set of 20 rotamers were generated for each alignment using Modeller9.19 (https://salilab.org/modeller/)[29]. The rotamer with the least sum of restraints (molpdf values) was selected from each set for further validation using different structure validation tools in SAVES server version 5 (https://servicesn.mbi.ucla.edu/SAVES/). The programs Verify3D[32,33], Errat[34,35], Prove (protein volume evaluation tool)[36] and Ramachandran plot[37] in SAVES server were applied on each of the six models. Inter-atomic clashes called short contacts were identified using Chimera 1.13.1[38]. Models were visualized using Pymol[39] and Chimera 1.13.1.

Sucrose and H^+ binding site prediction

Carbohydrate binding sites were predicted using a sequence-based Support vector machine (SVM) method provided by Sprint server (http://sparks-lab.org/server/SPRINT-CBH)[40]. Probable sucrose binding sites were defined as subsets of predicted carbohydrate binding sites having a prediction score value ≥ 0.1. Inward facing carbohydrate binding residues, identified using Chimera software were considered as the most likely sucrose binding residues. Potential H^+ binding residues are the negatively charged Asp and Glu residues in the second hexa helical bundle. Predicted sucrose and H^+ binding residues of OsSUT1 were mapped on to all the six OsSUT1 models using Chimera1.13.1.

Mutant sequence modelling

To test the effect of indels as well as synonymous/ non-synonymous mutations on OsSUT1, *in silico* mutations were introduced to the best model (Model 3). For this, the target-template alignment 3 was edited with the desired residue and 40 mutant rotamers for each mutation were generated using command line version of Modeller 9.19[29]. List of mutations are given in (Table 1). The mutant rotamer models were obtained by optimization of side chain confirmation of the mutant residues by energy minimization algorithm in Modeller.

Results and Discussion

Target-Template alignments and modelling

Two template folds lactose permease (PDB ID: 1PV7)[27] and YajR Transporter (PDB ID: 3wdo)[41] were selected for modelling from a set of structural folds identified by Phyre2 (with 100% confidence). From the sequence alignment between the template (1PV7) and the target (OsSUT1 Accession No: Q10R54.1) it was found that the large chunk of loop6 (connector between two hexa helix bundles) was not conserved between them except at the FRN-FRQ motifs at the loop boundary. It was also found that the SUT loop6 was longer than that of lactose permease (Suppl. File 1). Target-template sequence alignment is a crucial step in molecular modelling that determines the quality of the model generated[42]. Since the crystal structures of SUTs have not yet been solved, the closest available template was chosen for homology modelling despite its low sequence

Table 1 — List of *in silico* mutations on loop4 of OsSUT1 Model 3 and effect on knot formation

Sl No	Deletion/addition	Mutation	loop4 (in rice QGPARALMADLSGR)	Loop length	Knot
1	del1_nter_Q	Q137	GPARALMADLSGR	13	Absent
2	del2_nter_QG	Q137,G138	PARALMADLSGR	12	Absent
3	del3_nter_QGP	Q137,G138, P139	ARALMADLSGR	11	Absent
4	del4_nter_QGPA	Q137,G138, P139, A140	RALMADLSGR	10	Absent
5	del1_cter_R	R152	QGPARALMADLSG	13	present
6	del2_cter_GR	G151,R152	QGPARALMADLS	12	present
7	del3_cter_SGR	S150, G151,R152	QGPARALMADL	11	Absent
8	del4_cter_LSGR	L149,S150, G151, R152	QGPARALMAD	10	Absent
9	ins1_nter_Q	Q	QQGPARALMADLSGR	15	Absent
10	ins1_cter_R	R	QGPARALMADLSGRR	15	Present
11	subs1_nter_QN	Q137N	NGPARALMADLSGR	14	Present
12	subs2_nter_QV	Q137V	VGPARALMADLSGR	14	Present
13	subs3_nter_QD	Q137D	DGPARALMADLSGR	14	Present
14	subs4_nter_QR	Q137R	RGPARALMADLSGR	14	Present
15	subs5_nter_VG	V136G	GQGPARALMADLSGR	14	Present
16	subs7_nter_VL	V136L	LQGPARALMADLSGR	14	present
17	subs8_nter_VN	V136N	NQGPARALMADLSGR	14	present
18	subs9_nter_VQ	V136Q	QQGPARALMADLSGR	14	Present
19	subs10_nter_VD	V136D	DQGPARALMADLSGR	14	Present
20	subs11_nter_VR	V136R	RQGPARALMADLSGR	14	Present

*del=deletion, nter=N-terminal, cter=C-terminal, ins=insertion, subs=substitution

identity with OsSUT1. Low sequence identity can lead to mis-alignment resulting in gaps in the middle of TM helices which Modeller would wrongly model as a loop[29]. To remove such gaps we used refined alignments leading to five different models of OsSUT1. These models were validated further for identifying a reliable model for OsSUT1.

Structural validation of the models

Restraints calculation using Modeller 9.19

The restraint calculation of the rotamers generated by Modeller9.19 (Suppl. file 2) revealed that Model 3, Model 5 and Model 6 have the least mean sum of restraints (molpdf values) indicating the stability of these rotamers over the others. The mean molpdf values of the rotamers of these models were half of that of the raw alignment based Model 1 (Fig. 1) indicating the improvement in the stability of OsSUT1 models upon alignment refining.

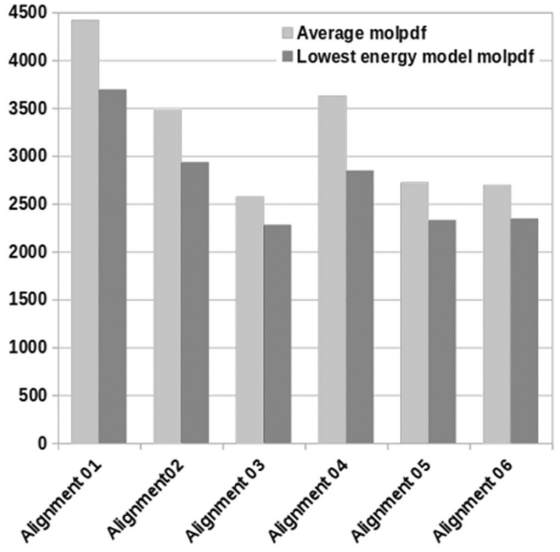

Fig. 1 — Mean molpdf values of 20 rotamers generated based on six different sequence-template alignments

Inter-atomic clashes

The refined alignment based models had fewer inter atomic clashes / short contacts (Fig. 2) compared to the raw alignment based model. The clashes mapped on to the structural models showed that the short contacts in model 1 (raw alignment) (Fig. 2A) and model 2 (Fig. 2B) were due to the wrong orientation of loops. These short contacts

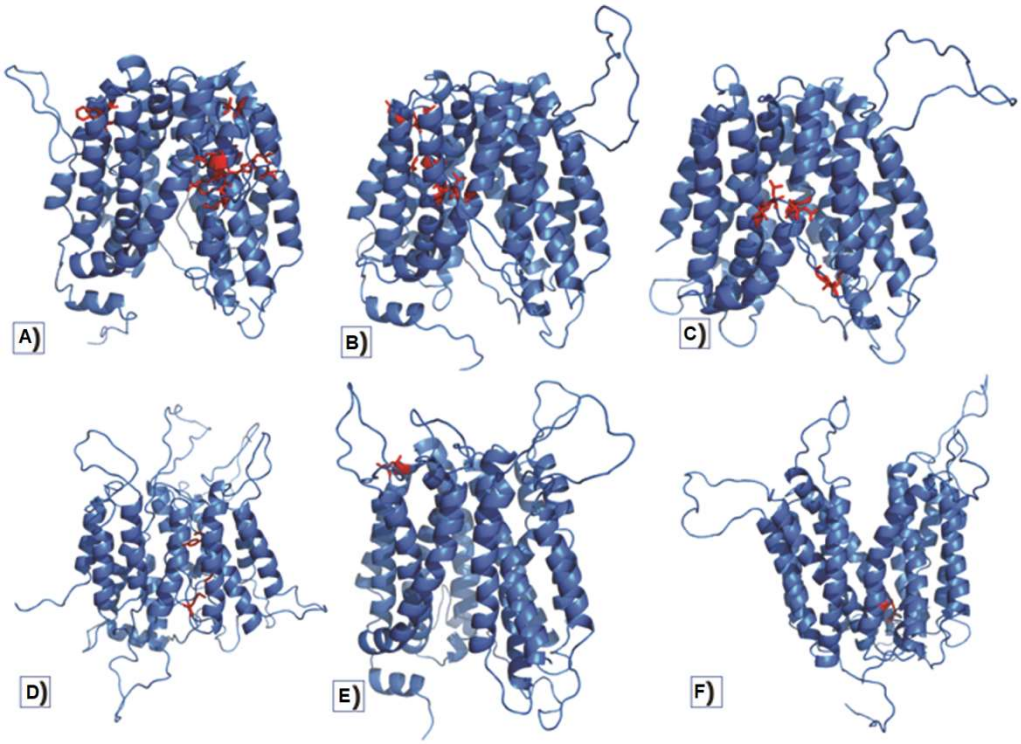

Fig. 2 — Inter-atomic clashes/short contacts (red) mapped on (A) model 1; (B) model 2; (C) model 3; (D) model 4; (E) model 5; and (F) model 6

were absent in model 3 for which loop boundaries were further redefined (Fig. 2C & Table 2). Among all, the Phyre2 alignment based models 5 and 6 showed the least number of short contacts (Fig. 2E & F).

Validation using SAVES server

For selecting the most likely OsSUT1 model, all the models were further evaluated using four parameters provided by the SAVES server. The first one was the 3D-1D alignment stability as predicted by verify3D program[32,33]. The 3D-1D alignment stability scores were high in models 3, 5 and 6 compared to the other models (Fig. 3A) implicating the correctness of these models. The second parameter is the Model quality by Errat module[34]. The overall model quality factor was highest for Model 2, 3 and 5 compared to the other models (Fig. 3B).

The third parameter, percentage buried atoms[36] in models 3, 5 and 6 were comparable to that of the templates indicating a minimal structural deviation from the templates (Fig. 4A). The fourth parameter, PHI-PSI angle distributions in the models 3, 5 and 6 were in the allowed regions of Ramachandran plot with minimal (less than 10) outliers (Fig. 4B, Suppl. File 3).

Comparative analysis of sucrose binding residues on select models 3, 5 and 6

Three models - Models 3, 5 and 6 – were selected based on structural validation with Modeller 9.19, Chimera and SAVES suit for comparative analysis of sucrose binding residues.

The predicted sucrose binding residues (Table 3 & Suppl. File 4) were mapped on the three select models to identify the best model. In the case of model 3 and model 6 the sucrose binding residues were distributed in the TM region (Fig. 5A & B), whereas in model 5, they were mostly dispersed at the periplasmic side and centre of TM region (Fig. 5C). In lactose permease, the lactose binding residues are known to be present in the TM region[27,43]. The positioning of the predicted sucrose binding residues within the channel on model 3 and 6 indicates the reliability of these models. Both the models 3 and 6 suggest the residues 63V, 67W, 111D and 177D to be sucrose binding (residue numbers as per rice sequence Q10R54.1, Table 3). Additionally, model 3 suggests 198H, and 332W as sucrose binding (Table 3).

Comparative analysis of probable H^+ channel residues

Further, we assessed the positions of putative H^+ binding sites on the select models. The acidic residues

(-vely charged) Asp and Glu are generally considered as potential H^+ binding sites[44]. The residues in the second half of the lactose permease are known to be involved in H^+ binding[27]. In line with this, the acidic residues in the second hexa-helical half of OsSUT1 were identified and mapped on to the three select models 3, 5 and 6 (Table 3 & Fig. 6A-C). The inward- facing H^+ binding residues in Model 3 are D329, E336, D346, E350 (residue numbers

Table 2 — Inter- atomic clashes as per chimera 1.13.1 structure analysis tool

Model	Number of Clashes	Clash details	Distance (Å)
1	9	TRP 272 CA-SER 429 O	2.667
		ASN168 CA-VAL 309 N	2.813
		ASN168 CA-GLY 308 CA	3.15
		ASN168 N-GLY 308 CA	2.857
		GLY175 CA-ALA 156 CA	2.916
		HIS151 CA-MET 166 CA	3.055
		LEU 22 CA-GLY 152 CA	2.879
		ARG 150 CA-GLN 17 O	2.669
		PHE 186 O-SER 211 CA	2.654
Model 2	8	GLU 446 CA-VAL431 O	2.669
		PRO 443 CA-VAL 431 N	2.823
		PRO 443 CA-VAL 431 CA	2.98
		TYR 281 CA – GLN 434 N	2.819
		TYR 281 N – GLN 434 N	2.671
		LEU 143 CA-GLY 370 CA	3.048
		LEU 143 N-GLY 370 CA	2.803
		MET 144 N-ALA 313 CA	2.802
Model 3	5	GLY 370 CA-LEU143 N	2.797
		ALA313 CA-MET144 N	2.819
		GLY 312 CA-ASP 146 CA	2.951
		GLY 152 CA-GLN 137 CA	3.046
		GLY 152 CA-GLY 138 N	2.904
Model 4	3	GLY156 CA-MET 148 CA	3.086
		GLY 301 CA-Gly 142 CA	2.942
		Gly 297 CA-TYR 19 CA	2.993
Model 5	1	LEU 357 N-GLY 449 CA	2.823
Model 6	1	GLN 425 CA-THR 429 N	2.822

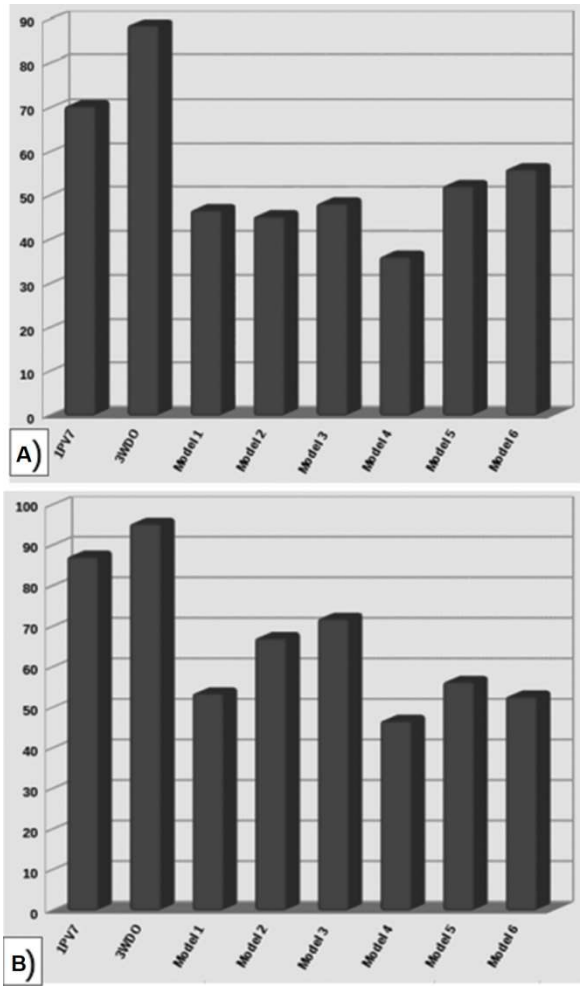

Fig. 3 — (A) 3D-1D alignment stability scores for different models as calculated by Verify3D; and (B) Overall model quality factor for different models as calculated by Errat program.

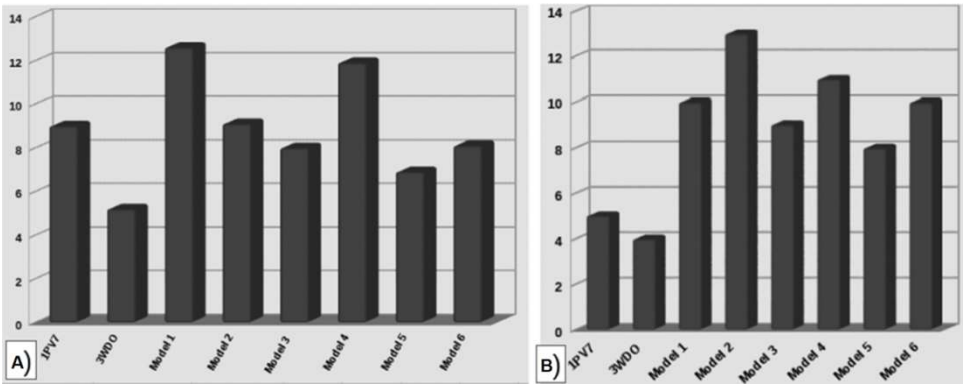

Fig. 4 — (A) percentage buried atoms in different models as calculated by Prove Program; and (B) Number of outliers in Ramachandran plot of residues in the Models

as per rice sequence Q10R54.1, Table 3). In model 3 they were dispersed at the periplasmic side as well as transmembrane region (Fig. 6A) similar to that in lactose permease. In model 5 and 6 (Figs. 6C and 7), they were found in the periplasmic or cytoplasmic sides only. Model 3 which showed H^+ binding sites as well as sucrose binding sites within the channel, therefore, was considered as the most probable model of OsSUT1. The H^+ binding residue E336 was found to be placed at the centre interacting with the sucrose binding sites of the channel (Fig. 7). Thus model 3 suggests a mechanism of sucrose transport by binding to the site at the centre of TM channel that is accessible from both the sides of the membrane similar to that in lactose permease[42].

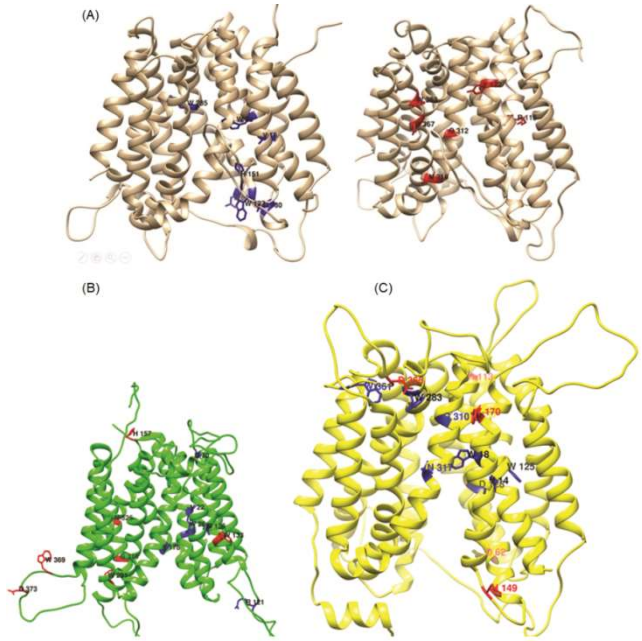

Fig. 5 — Carbohydrate binding residues above score 0.1 (A) inward– facing (blue); and (B) outward– facing (red) in model 3, model 5 and model 6

In silico mutations on OsSUT1 Model 3

Model 3 showed a strong interaction between QGP(X)R(X)$_4$D motif of loop4 and GVR-G-L-L-NS motif of helix VIII forming a knot. The knot was found to be stabilized by hydrophobic and salt

Table 3 — Putative sucrose binding site amino acids with score >0.1

Residue number in OsSUT1 sequence (Accession No. Q10R54.1)	Equivalent residue in Model 3	Equivalent residue in Model 5	Equivalent residue in Model 6
V63	V16	V14	V22
W67	W20	W18	W26
D111	D64	D62	D70
W174	W127	W125	W133
D177	D130	D128	D136
H198	H151	H149	H157
W332	W285	W283	W291
R162	R115	R113	R121
Y219	Y172	Y170	Y178
G359	G312	G310	G318
N366	N319	N317	N325
W410	W363	W361	W369
D414	D367	D365	D373
Putative H^+ binding residues in OsSUT1			
D329	D282	D280	D288
D331	D284	D282	D290
E336	E289	D287	D295
D341	D294	D292	D300
D346	D299	D297	D305
E350	E303	E301	E309
E378	E331	E329	E337
D414	D367	D365	D373
D426	D379	D377	D385
D492	D445	D443	D451
E493	E446	D444	E452

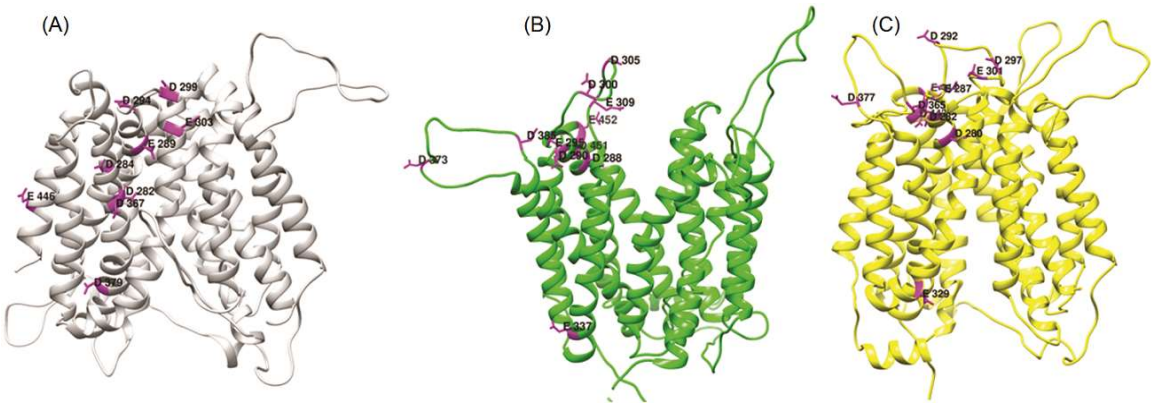

Fig. 6 — Putative H^+ binding sites on model 3, model 5 and model 6

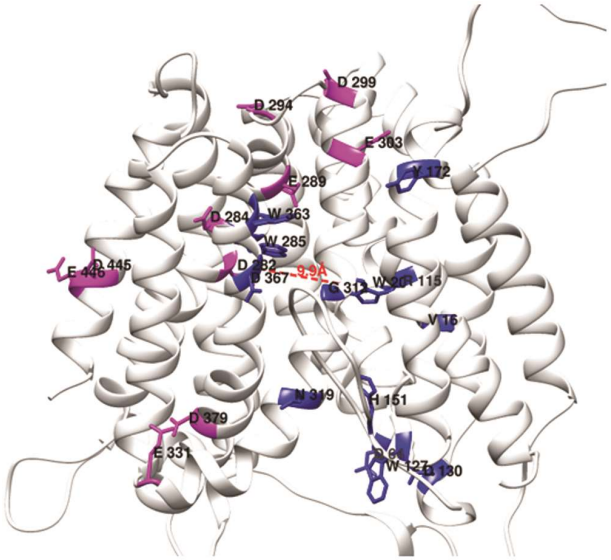

Fig. 7 — Probable Sucrose and H^+ binding site residues mapped on model 3

bridge interactions between Asp 193 (D145 of QGPARALMADL) and Asn319 (N366 of GVRAGALLL**N**S) placed at a distance of 3.8 Å (Suppl. File 5). In raw alignment model where the knot is absent, these residues were placed at 10.8 Å. It is possible that these two motifs interact to bring the two hexa helical halves of SUT1 closer forming the sucrose/H^+ channel. The OsSUT1 mutant R188K (QGP(X)R$(X)_4$D motif) failed to transport sucrose and showed an H^+ leak implicating the functional importance of this motif[26].

The knot formation could be loop length dependent as suggested by the absence of knot in the N and C terminal deletion mutants (Table 1). The loop length and loop sequence are indeed known to determine knot formation[45]. Further, a single residue deletion (del1_nter_Q), in which Q137 of the highly conserved QGP motif was removed, did not show knot structure indicating the functional importance of QGP motif. In a previous study using split ubiquitin system, it was suggested that the two halves of SUT indeed interact and results in homo or hetero dimer[8]. The current study suggests an intra molecular interaction between the QGP containing loop 4 and GVRAGALLL**N**S motif facilitating the formation of sucrose/H^+ channel.

Conclusion

In this study, a refined target template alignment was used for structural modelling of OsSUT1. This alignment refining resulted in a reliable homology model of OsSUT1. The proposed model obtained by threading followed by comparative modelling as suggested for twilight zone templates act as a base for point mutation experiments. The study provides insights on intra molecular interactions in SUTs and identifies residues that are most likely involved in sucrose/H^+ symport.

Conflict of interest

All authors declare no conflict of interest.

Acknowledgement

Authors thank Science and Engineering Research Board, Govt of India for funding (Grant No YSS/2015/001916)

References

1 Scofield GN, Hirose T, Aoki N & Furbank RT, Involvement of the sucrose transporter OsSUT1 in the long-distance pathway for assimilate transport in rice. *J Exp Bot*, 58 (2007) 3155.

2 Pao SS, Paulsen IT & Saier AH Jr, Major facilitator super family. *Microbiol Mol Biol Rev*, 62 (1998) 1.

3 Riesmeier JW, Hirner B & Frommer WB, Potato sucrose transporter expression in minor veins indicates a role in phloem loading. *Plant Cell*, 5 (1993) 1591.

4 Liesche J, Sucrose transporters and plasmodesmal regulation in passive phloem loading. *J Integr Plant Biol*, 59 (2017) 311.

5 Ludewig F & Flügge UI, Role of metabolite transporters in source–sink carbon allocation. *Front Plant Sci*, 4 (2013) 231.

6 Carpaneto A, Geiger D, Bamberg E, Sauer N, Fromm J & Hedric R, Phloem-localized proton-coupled sucrose carrier ZmSUT1 mediates sucrose efflux under the control of the sucrose gradient and the proton motive force. *J Biol Chem*, 280 (2005) 21437.

7 Lalonde S, Wipf D, Frommer WB Transport mechanisms for organic forms of carbon and nitrogen between source and sink. *Annu Rev Plant Biol*, 55 (2004) 341.

8 Reinders A, Schulze W, Thaminy S, Stagljar I, Frommer WB & Ward JM, Intra and inter molecular interactions in sucrose transporters at the plasma membrane detected by the split-ubiquitin system and functional assays. *Structure*, 10 (2002)763.

9 Bush DR, Electrogenicity, pH-dependence and stoichiometry of the proton–sucrose symport. *Plant Physiol*, 93 (1990) 1590.

10 Naik A, Dandekar S & Naik N, Effect of Indian honey on expression of p53 and cyclin B1 in HeLa cells. *Indian J Biochem Biophys*, 57 (2020) 178.

11 Barker L, Kühn C, Weise A, Schulz A, Gebhardt C, Hirner B, Hellmann H, SchulzeW, Ward JM & Frommer WB, SUT2, a Putative Sucrose Sensor in Sieve Elements. *Plant Cell*, 1 (2000)1153.

12 Sivitz AB, Reinders A, Johnson ME, Krentz AD, Grof CPL, Perroux JM & Ward JM, Arabidopsis sucrose transporter AtSUC9, high-affinity transport activity, intragenic control of expression, and early flowering mutant phenotype. *Plant Physiol*, 143 (2007) 188.

13 Xu Q, Chen S, Yunjuan R, Chen S & Liesche J, Regulation of sucrose transporters and phloem loading in response to environmental cues. *Plant physiol*, 176 (2018) 930.

14 Usha B, Bordoloi D & Parida A, Diverse expression of sucrose transporter gene family in Zea mays. *J Genet*, 94 (2015) 151.

15 Biswas S, Mahapatra E, Roy M & Mukherjee S, PEITC by regulating Aurora Kinase A reverses chemoresistance in breast cancer cells. *Indian J Biochem Biophys*, 57 (2020) 167.

16 Hirose T, Endler A & Ohsugi R, Gene expression of enzymes for starch and sucrose metabolism and transport in leaf sheaths of rice (*Oryza sativa* L.) during the heading period in relation to the sink to source transition. *Plant Prod Sci*, 2 (1999) 178.

17 Aoki N, Hirose T, Scofield GN, Whitfeld PR & Furbank RT, The sucrose transporter gene family in rice. *Plant Cell Physiol*, 44 (2003) 223.

18 Wang L, Lu Q, Wen X & Lu C, Enhanced sucrose loading improves rice yield by increasing grain size. *Plant Physiol*, 169 (2015) 2848.

19 Scofield GN, Aoki N, Hirose T, Takano M, Jenkins CL & Furbank RT, The role of the sucrose transporter, OsSUT1, in germination and early seedling growth and development of rice plants. *J Exp Bot*, 58 (2007) 483.

20 Al-Sheikh Ahmed S, Zhang J, Ma W & Dell B. Contributions of TaSUTs to grain weight in wheat under drought. *Plant Mol Biol*, 98 (2018) 333.

21 Slewinski TL, Meeley R & Braun DM, Sucrose transporter1 functions in phloem loading in maize leaves. *J Exp Bot*, 60 (2009) 881.

22 Leach KA, Tran TM, Slewinski TL, Meeley RB & Braun DM, Sucrose transporter2 contributes to maize growth, development, and crop yield. *J Integr Plant Biol*, 59 (2017) 390.

23 Cai Y, Tu W, Zu Y, Yan J, Xu Z, Lu J & Zhang Y, Over expression of a grapevine sucrose transporter (VvSUC27) in tobacco improves plant growth rate in the presence of sucrose *in vitro.* Front *Plant Sci*, 8 (2017) 1069.

24 Riesmeier JW, Willmitzer L & Frommer WB Anti-sense repression of the sucrose transporter affects assimilate partitioning in transgenic potato plants. *EMBO J*, 13 (1994) 1.

25 Yan N, Structural advances for the major facilitator superfamily (MFS) transporters. *Trends Biochem Sci*, 38 (2013) 151.

26 Sun Y & Ward JM, Arg188 in rice sucrose transporter OsSUT1 is crucial for substrate transport. *BMC Biochem*, 13 (2012) 26.

27 Abramson J, Smirnova I, Kasho V, Verner G, Kaback HR & Iwata S, Structure and mechanism of the lactose permease of *Escherichia coli. Science*, 301 (2003) 610.

28 Kelley LA, Mezulis S, Yates CM, Wass MN & Sternberg MJ, The Phyre2 web portal for protein modeling, prediction and analysis. *Nat Protoc*, 10 (2015) 845.

29 Sali A & Blundell TL, Comparative protein modelling by satisfaction of spatial restraints. *J Mol Biol*, 234 (1993) 779.

30 Thompson JD, Higgins DG & Gibson TJ, Clustal W: improving the sensitivity of progressive multiple sequence alignment through sequence weighting, position-specific gap penalties and weight matrix choice. *Nucleic Acids Res*, 22 (1994) 4673.

31 Waterhouse AM, Procter JB, Martin DMA, Clamp M & Barton GJ, Jalview Version 2 – A multiple sequence alignment editor and analysis workbench. *Bioinformatics*, 25 (2009) 1189.

32 Bowie JU, Lüthy R & Eisenberg D, A method to identify protein sequences that fold into a known three-dimensional structure. *Science*, 253 (1991) 164.

33 Lüthy R, Bowie JU & Eisenberg D, Assessment of protein models with three-dimensional profiles. *Nature*, 356 (1992) 83.

34 Colovos C & Yeates TO, Verification of protein structures: patterns of nonbonded atomic interactions. *Protein Sci*, 2 (1993) 1511.

35 Mishra AK, Pandey B, Tyagi C, Chakraborty O, Kumar A & Jain AK, Structural and functional analysis of Chitinase gene family in wheat (*Triticum aestivum* L.). *Indian J Biochem Biophys*, 52 (2015) 169.

36 Pontius J, Richelle J & Wodak SJ, Deviations from standard atomic volumes as a quality measure for protein crystal structures. *J Mol Biol*, 264 (1996)121.

37 Ramachandran GN, Ramakrishnan C & Sasisekharan V, Stereochemistry of polypeptide chain configurations. *J Mol Biol*, 7 (1963) 95.

38 Pettersen EF, Goddard TD, Huang CC, Couch GS, Greenblatt DM, Meng EC & Ferrin TE, UCSF Chimera - A visualization system for exploratory research and analysis. *J Comput Chem*, 25 (2004) 1605.

39 DeLano WL, Pymol: An open-source molecular graphics tool. *CCP4 Newsletter on Protein Crystallography*, 40 (2002) 82.

40 Taherzadeh G, Zhou Y, Liew AW & Yang Y, Sequence based prediction of protein-carbohydrate binding sites using support vector machines. *J Chem Inf Model*, 56 (2016) 2115.

41 Jiang D, Zhao Y, Wang X, Fan J, Heng J, Liu X, Feng W, Kang X, Huang B, Liu J & Zhang XC, Structure of the YajR transporter suggests a transport mechanism based on the conserved motif A. *Proc Natl Acad Sci U S A*, 110 (36) (2013) 14664.

42 Barbato A, Benkert P, Schwede T, Tramontano A & Kosinski J, Improving your target-template alignment with MO Dalign. *Bioinformatics*, 28 (2012) 1038.

43 Kaback RH Structure and mechanism of the lactose permease. *Comptes Rendus Biologies*, 328 (2005) 557.

44 Smith ES, Zhang X, Cadiou H & McNaughton PA, Proton binding sites involved in the activation of acid-sensing ion channel ASIC2a. *Neurosci Lett*, 426 (2007) 12.

45 Potestio R, Micheletti C & Orland H, Kotted vs unknotted proteins: evidence of knot promoting loops. *Plos Comput Biol*, 6 (2010) e1000864.